SCIENCE CHINA
Technological Sciences

December 2011 Vol.54 Suppl. 1: 1–8
doi: 10.1007/s11431-011-4625-4

Simulation of influence of multi-defects on long-term working performance of high arch dam

ZHANG GuoXin*, LIU Yi, ZHENG CuiYing & FENG Fan

State Key Laboratory of Simulation and Regulation of Water Cycle in River Basin, Beijing 100038, China;
China Institute of Water Resources and Hydropower Research, Beijing 100038, China

Received July 11, 2011; accepted October 8, 2011; published online November 15, 2011

As an integrated structure, an arch dam is assumed to bear loads in its design consideration. However, multi-defects, such as cracks and the opening of transverse joints, are unavoidable during construction and operation. Multi-defects will reduce the structural integrity and stiffness of the dam and affect its working performance and degree of safety. In the current paper, a numerical model of defects and a simulation method of a high arch dam are introduced. The Chencun arch dam is analyzed as a case study. An entire course simulation analysis of the Chencun arch dam from construction to operation is carried out, through which the opening of the transverse and longitudinal joints, formation of cracks, and their influence on deformation and stress of the dam are studied. According to the results of the analysis, appropriate measures should be adopted to prevent the development of cracks, and observation should be strengthened for a more timely discovery of risks.

high arch dam, crack, multi-defects, working performance

Citation: Zhang G X, Liu Y, Zheng C Y, et al. Simulation of influence of multi-defects on long-term working performance of high arch dam. Sci China Tech Sci, 2011, 54(Suppl. 1): 1–8, doi: 10.1007/s11431-011-4625-4

1 Introduction

The 240 m Ertan arch dam in China has been in operation for more than 10 a. Several super-high arch dams, such as the Xiaowan, Laxiwa, and Goupitan, have been completed successively, indicating that the construction technology for super-high arch dams in China has continued to mature. However, despite these developments, the history of "no dam without cracks" has not ended because the problem of cracks still persists. Cracks in concrete occur mainly during the construction period, with most of the cracks appearing on the placement surface, upstream and downstream surfaces, and side surfaces. After proper repair, these cracks still exert some influence on dam safety. Some dams have experienced large-scale cracks. For example, the Chencun dam, which was completed in 1960s, has a great number of long and deep cracks on the dam crest and horizontal cracks on downstream surface, with some cracks penetrating through many dam monoliths. In another high dam in Southern China, a large crack parallel to the dam axis and 1/3 dam thickness away from the upstream was found during construction. The crack penetrated six to seven monoliths, with the total area of cracks accounting for 7% of the upstream surface area. A recently built super high arch dam also has serious cracks. Some arch dams begin to have cracks after several years of operation. For instance, 49 cracks were found on an RCC dam [1] after 3–4 a of operation, with 2 cracks going through upstream and downstream surfaces. Many cracks have also appeared on a super-high arch dam after five to six years of operation. In addition, the opening of grouted transverse joints occurred in many dams.

*Corresponding author (email: zhanggx@iwhr.com)

Once an arch dam is formed after closure grouting, gravity, water pressure, and temperature all exert load on both the beams and arches. After grouting, small cracks have little effect on the integrity of the dam, but large cracks and opened transverse joints can influence the overall stability of the dam. According to results of the overloading test of water pressure, if the defects of transverse joints, longitudinal joints, and cracks are not considered, the overload safety factor of Chencun dam is 4.0. However, if the defects are taken into account, based on the simulation analysis, the safety factor of Chencun dam can be as low as 1.8–1.91, indicating that the defects may substantially reduce the overall safety of the dam. The influence of defects may be included as a safety factor in the assessment of arch dams with heights lower than 200 m. However, for super-high arch dams, because of the huge water load and high stress level, the influence of defects that can cause significant damage or even failure cannot be simply included under the same safety factor. The analysis methods, design theories, and experiences obtained from the common arch dam cannot be applied to super-high arch dams. Many arch dams in other countries have also suffered serious cracks, for instance, Zeuzier and Zervreila in Switzerland, Sayan-Shushensk in the former Soviet Union, and Zillergrundl in Austria. The Kolnbrein dam in Austria, which has serious cracks, is a good example of a high arch dam with damage from cracks. Many experts believe that the cracks on the dam heel are closely related to the high stress level [2–4].

The numerical method is one of the major methods for studying the stress and safety of arch dams [5, 6]. The key point in the numerical analysis of arch dams with defects is the simulation of cracks and transverse joints. There are many models on the simulation of concrete cracks, including discrete model, smeared-crack model, thin layer element model, and contact model. A typical model of the discrete model was by Ngo [7], Hillerborg et al. [8] and Bazant et al. [9] proposed the smeared-crack model. Thereafter, many scholars conducted studies to improve these models [10]. The discrete and smeared-crack models are used mainly to simulate the crack propagation of several cracks. Based on the non-thickness joint element by Goodman (Goodman element), the thin layer element model has been developed into a thin element with thickness [11] and shear dilatation joint element [12], which can only be used for small deformations, with the upper and lower surfaces as well as the corresponding point pairs forming into an element and the relationship between point pairs remaining unchanged. In the contact model, the relationship between the point pairs is replaced by the parallelism relationship of points and face, varying with the deformation [13] in order for a large deformation to be calculated. Its constitutive relation is different from that of cracks because keys are set on transverse joints. The opened cracks cannot transfer shear force; rather, after closing, the shear transfer depends on the parameters of the shear strength of the joint faces. In contrast, the transverse joints can transfer the shearing forces, and the transfer capability depends on the relationship of the surface set with keys. Zhu [14] proposed a keyway element with thickness to simulate the transverse joints, whereas Li [15], Li et al. [16], Zhang et al. [17], Long et al. [18], and Zhang et al. [19] conducted analyses of the stress characteristics of an arch dam considering the keyways.

Many research results have been achieved on the simulation of the deformation and stress of dams with several cracks under monotonic and earthquake loadings. In long-term operations, dams will periodically act under the loads of water pressure and temperature. During this period, the cracks and transverse joints may open or close, some cracks will develop further, and some new cracks may appear. Therefore, this process is a coupling of the geometric nonlinearity, contact nonlinearity, and material nonlinearity. For the nonlinear interaction of cracks and transverse joints, the simulation of long-term stress and deformation under periodic loading is the key problem that needs to be addressed. The current paper discusses the simulation method of the open-close state of cracks and transverse joints under all the loads and nonlinear problems such as sliding yielding. Corresponding software has been developed to simulate the deformation and stress characteristics of arch dams.

2 Simulation method of arch dam with defects

1) Definition of joint element [20]

In the current paper, a joint element refers to crack and transverse joint elements. These two types of joints are different in their constitutive relations but are similar in the definition of displacement function and stiffness matrix. For cracks on the spatial surface, they can be defined by 8–20 joint-varying thin-layer elements, as shown in Figure 1.

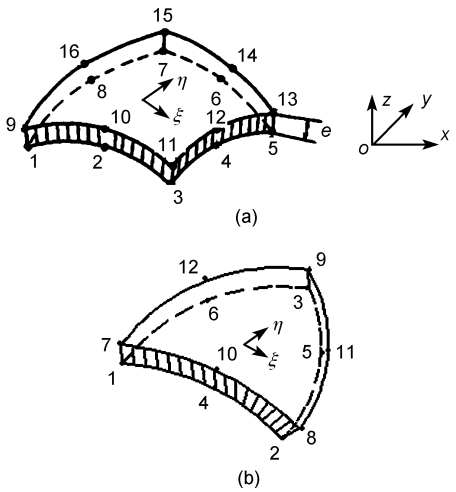

Figure 1 Joint element with a curved surface. (a) Quadrilateral element; (b) triangle element.

The deformation at any point of the joint surface is

$$\begin{bmatrix}\Delta u\\ \Delta v\\ \Delta w\end{bmatrix}=\sum_{i=1}^{N}[N_i]\begin{bmatrix}u_i\\ v_i\\ w_i\end{bmatrix}, \tag{1}$$

where $[N_i]$ refers to the shape function. The stiffness matrix of the joint element is

$$[k]^e=\int_{-1}^{1}\int_{-1}^{1}[N]^{\mathrm{T}}[L]^{\mathrm{T}}[D][L][N]\mathrm{d}\xi\mathrm{d}\eta, \tag{2}$$

where $[L]$ is the coordinate transformation matrix, and $[D]$ is the elastic matrix.

When the joints yield/open and the normal force/shear stress on joint surface needs to be released, the non- balanced force of the released stress is calculated according to the following equation:

$$[P]^e_{\sigma_0}=-\int_{-1}^{1}\int_{-1}^{1}[N]^{\mathrm{T}}[L]^{\mathrm{T}}\left[\sigma_0^{'}\right]|J|\mathrm{d}\xi\mathrm{d}\eta. \tag{3}$$

Local opening or yielding of the joint can be defined through the Gauss point and can be reflected through the adjustment of the normal and tangential stiffness of the integral point in eqs. (2) and (3).

2) Elastic coefficient matrix of joint element

i) Matrix $[D]$ in the general definition of eq. (2) is the elastic matrix of joint element. By changing the value of the matrix, different joints and their states can be simulated. It is defined by the following equation:

$$[D]=\begin{bmatrix}K_s & 0 & 0\\ 0 & K_s & 0\\ 0 & 0 & K_n\end{bmatrix}=\frac{1}{e}\begin{bmatrix}G_s & 0 & 0\\ 0 & G_s & 0\\ 0 & 0 & G_n\end{bmatrix}, \tag{4}$$

where e is the element thickness, and G_s and G_n refer to the shear modulus of the interior materials of joint elements along the tangential direction and elastic modulus along the normal direction, respectively. When the thickness of joint element is 0, the computation equation is

$$[D]=\begin{bmatrix}\lambda_s & 0 & 0\\ 0 & \lambda_s & 0\\ 0 & 0 & \lambda_n\end{bmatrix}, \tag{5}$$

where λ_s and λ_n are the normal and tangential stiffnesses of the joint surface. Their values are adopted according to test results; if there are no test values available, a larger value is taken to express the deformation of joint surface and to avoid penetration error.

ii) Constitutive relation of the dentate keyslot.

The states of the dentate keyslot are shown in Figure 2.

If δ_n is used to express the accumulated opening in the normal direction, and δ_h is the tangential displacement, then the state of joints has three types:

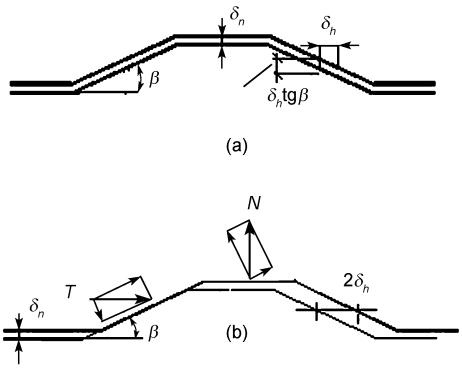

Figure 2 Dentate keyslot. (a) Opening; (b) lateral clutch.

a) $\delta_n \leqslant 0$, close: $\alpha_h=1$, $\alpha_n=1$;

b) $\delta_n>0$, $|\delta_h|<\delta_n\mathrm{ctg}\beta$, open: $\alpha_h=0$, $\alpha_n=0$;

c) $\delta_n>0$, $|\delta_h|\geqslant\delta_n\mathrm{ctg}\beta$, open: the side surfaces of keyslot come into contact $\alpha_h=2.5\xi\sin\beta$, $\alpha_n=\xi\cos\beta$.

α_h and α_n are the modification coefficients of stiffness in the tangential and normal directions, respectively. ξ is the area ratio of the side of the keyslot to the transverse joint. The elastic matrix is revised as follows:

$$[D]^{'}=\begin{bmatrix}\alpha_h^x K_{\mathrm{s}} & 0 & 0\\ 0 & \alpha_h^y K_{\mathrm{s}} & 0\\ 0 & 0 & \alpha_n K_n\end{bmatrix}. \tag{6}$$

iii) Spherical keyslot.

Spherical keyslots were first adopted in the Ertan arch dam and have since been widely used in super-high arch dams, such as Xiaowan, Jinping I, and Xiluodu. Its design is shown in Figure 3.

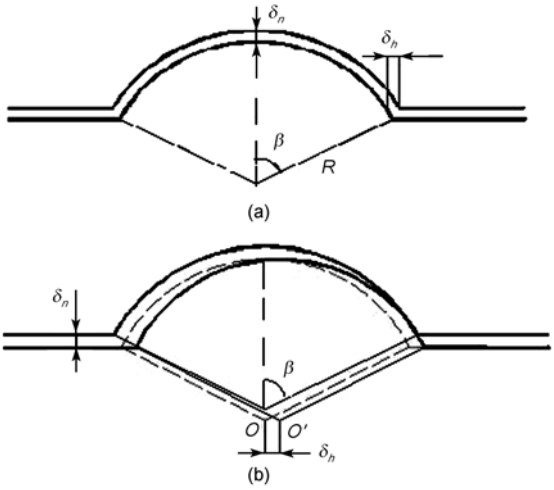

Figure 3 Spherical keyslot. (a) Opening; (b) lateral clutch.

Spherical keyslots have three states:

a) $\delta_n \leqslant 0$, close, $\alpha_h = 1$, $\alpha_n = 1$;

b) $\delta_h > 0$, $|\delta_h| < R\sin\beta - \sqrt{R^2\sin^2\beta - 2R\delta_n\cos\beta - \delta_n^2}$, open: $\alpha_h = 0$, $\alpha_n = 0$;

c) $\delta_n > 0$, $|\delta_h| \geqslant R\sin\beta - \sqrt{R^2\sin^2\beta - 2R\delta_n\cos\beta - \delta_n^2}$, open: side surfaces of the keyslot come into contact: $\alpha_h = 2.5\xi\sin\beta$, $\alpha_n = \xi\cos\beta$.

3) Simulation of joint failure

The joint state depends on tensile and shear strengths. When the stress is lower than the failure strength, the joint is in cohesion, and the load transferring mechanism is consistent with that without joints. However, when the stress outreaches the failure strength, the joint fails. The strength criterion of joints is as follows:

i) tensile failure $\sigma_n > \sigma_c$,

ii) shear failure

compressive shear $\tau > c + \sigma_n \mathrm{tg}\phi$,

tensile shear $\tau > c$,

iii) compressive shear and sliding $\tau > c' + \sigma_n \mathrm{tg}\phi'$,

where σ_c is the tensile strength of joints, c is the cohesion, ϕ is the friction angle, and c' and ϕ' are the residual cohesion and residual friction angle, respectively.

4) Opening and closing of joints and simulation of sliding

In the operation period, the arch dam is influenced by the periodic variation of temperature and water pressure. Thus, the state of joints constantly changes because of cyclic loading. For example, some joints open in winter and close in summer, whereas others act reversely. The same joint may open and close repeatedly under the influence of temperature and water level changes. Moreover, the opening and closing of many joints interact with each other. Some joints may also have reciprocating shear sliding. Therefore, the opening-closing and sliding of multiple joints are nonlinear problems. Shi et al. [10] considered it a high- dimensional non-linear problem that can be solved by the non-linear iterative method.

By referring to the non-linear iterative method proposed by Shi Genhua, the current paper tries to solve the problems of opening-closing and sliding of joints. As the variations of temperature and water level are simulated, the incremental method is adopted to simulate loads. The total increment method is used to simulate the state of opening and closing and sliding.

The changes in the state and calculation method of joints between Step i and Step $i+1$ are shown as follows:

a) From close to close without sliding yield: No treatment of the stiffness matrix is required, and there is no need to release the non-balanced force.

b) From close to close with yield sliding, i.e., shear strength $|\tau| > c + \sigma_n \tan\phi$, Stiffness coefficient: $\alpha_n^i \to \alpha_n^{i+1}$, $\alpha_h^i \to \alpha_h^{i+1} = 0$; $\alpha_h^i \to \alpha_h^{i+1} = 0$.

c) There are two scenarios from close to open:

i) For general cracks or keyways with shear failure or sides that are not in contact:

Stiffness coefficient: $\alpha_n^i \to \alpha_n^{i+1} = 0$, $\alpha_h^i \to \alpha_h^{i+1} = 0$;

Release all the stress on joint face in Step *i*.

ii) For keyways without shear failure and whose sides are in contact:

Stiffness coefficient: $\alpha_n^i \to \alpha_n^{i+1}$, $\alpha_h^i \to \alpha_h^{i+1}$;

Release the normal force and shear stress in Step *i*.

d) From open to close.

In the previous step, the normal opening is "+", whereas in the present step, it is "–". Calculating the tangential penetrating proportion to determine the tangential force for complementation is necessary. Stiffness coefficient: $\alpha_h^i \to \alpha_h^{i+1}$, $\alpha_n^i \to \alpha_n^{i+1}$

Stress needs to be complemented:

$$[\sigma']^e = [D]\begin{bmatrix}\delta_x' \\ \delta_y' \\ \delta_n'\end{bmatrix},$$

where δ_n' is the penetration in the normal direction, and δ_x' and δ_y' refer to the displacement in the directions of the local coordinate x' and y' after the penetration of the contact point.

In one loading time step, all the joint elements undergo repeated alternation in accordance with states from a)–d) until convergence is obtained. They then move on to the next loading time step.

5) Program development

The joint model and simulation methods introduced in the current paper are added to the simulation software SAPTIS, which is used for temperature and stress analysis, to develop an analysis tool with comprehensive functions. With the developed software, the excavation of dam foundation, concrete pouring, water cooling, grouting, impoundment by stage, temperature and influence on the dam caused by water level variation can be simulated. The temperature, stress, deformation and working performance of the dam from construction to operation can also be simulated to evaluate the safety of the dam. This method has been successfully utilized in the simulation analysis of high arch dams, such as Ertan, Xiaowan, Xiluodu, Jinping I and Laxiwa.

3 Simulation of the long-term working performance of the Chencun arch dam

1) Introduction

The Chencun hydropower station is located on the Qingyi River in Jing County, Anhui Province. The reservoir has a storage capacity of 2.476 billion m^3. The project mainly

consists of a concrete gravity arch dam, left and right spillways on the dam crest, middle outlet for flood discharge, bottom outlet, and a power house at the dam heel. The dam has a maximum height of 76.3 m, a dam crest width of 8 m, and a maximum bottom width of 53.2 m. The dam is divided into 28 blocks, and the arch length at the dam crest is 419 m.

The construction of the Chencun dam began in 1958 and lasted for 20 a, with impounding starting in 1982. The construction of stage I began in 1958 and ended in 1962; stage II began in 1968; and the main works were completed in 1972. In 1978, the dam was given an additional height of 1.3 m. Due to the long period of concrete placement between stages I and II and because less attention was paid to the temperature control measures, the concrete of the dam had poor quality. Moreover, complex geological and typographic conditions made the stress of the dam more complicated. During the construction and operation period, many cracks appeared on the dam. The horizontal crack near EL105m at the downstream surface crossed 24 dam blocks at more than 300 m long. The depth of the crack on the riverbed blocks was more than 5 m. The horizontal cracks, which crossed 16 dam blocks at a depth of more than 12 m, was distributed near EL111.5m at the downstream surface. Longitudinal cracks were also detected at EL105m of the inspection gallery and dam crest at a depth of over 8 m. The distribution of the major cracks on the dam section is presented in Figure 4. The open-close state of the crisscross cracks varies with the variations of temperature and water level, influencing the working performance and safety of the dam.

2) Computation model

To consider the conditions during the construction and operation of Chencun arch dam and simulate the process of crack development, the entire period from construction to operation was simulated. Taking into account the main factors affecting the stress and deformation of the dam comprehensively, the established three-dimensional finite element model considered over-flow blocks, diversion tunnels, mid and bottom outlets, sluice piers, and other complex structures.

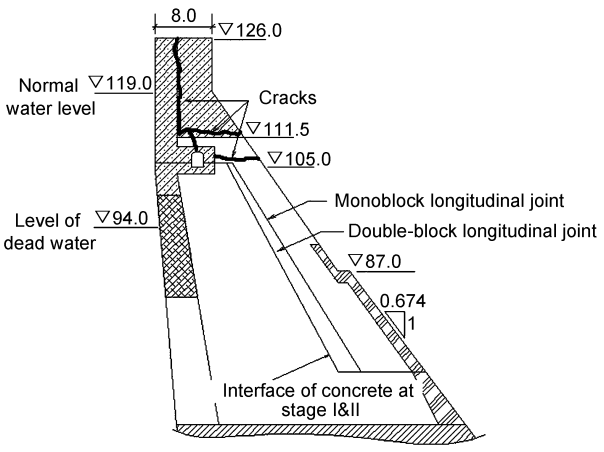

Figure 4 Illustration of the cross section and main cracks.

In the simulation analysis, recorded air temperature, water temperature, and water level were used as boundary conditions, based on which the entire course of construction and operation of the dam was simulated. The simulated factors include the recorded construction data of concrete, such as pouring time, placing temperature of concrete, and water pipe cooling information; grouting of transverse joints; and impounding and operation process. Figure 5 shows the simulation process of placement and grouting. Figure 6 shows the changes in air temperature and water level. All transverse and longitudinal joints and main cracks were considered in the model shown in Figure 7. The changes in the adiabatic temperature rise of concrete, elastic modulus, and creep along with ages were considered in the simulation analysis. The computation period started from September 23, 1959, when the first concrete was placed, until December 2004. In the placement process, the minimum computation step was 0.5 d, and the maximum step was 5 d. In the long duration of the placement, the minimum computation step was 0.5 d, and the maximum step was 30 d. There were 1801 computation steps in the simulation process.

3) Back analysis of the parameters

The major parameters are shown in Table 1. To simulate the real working performance, the parameters used in the simulation analysis should be determined through back analysis with observed data. In the current paper, the temperature and displacement fields of a typical section were analyzed using different parameters, such as the elastic modulus and coefficient of temperature conductivity. The correlation functions between the error and the parameters were built according to the observed data. Finally, the correct parameter, in which the error is the smallest, was selected. The adiabatic temperature rise in concrete for different gradations was determined according to the practical mix ratio of concrete recorded and the maximum internal temperature observed on site. The other parameters were determined by referring to similar projects.

4) Process and state of crack development

The initial strength of joints was set as shown in Table 2. The development of cracks was modeled through the simulation analysis.

The formation and development of cracks and joints obtained are shown in Figure 8.

Figure 8 shows that most of the longitudinal joints failed in the first one to two years after the placement of stage II concrete; this failure was the result of excessive tensile stress caused by the temperature drop. About 81% of the longitudinal joints failed during the long period of operation. According to construction records, grouting of transverse joints was not conducted above EL110m; the grouting of the joints below EL110m began in 1969 and was completed

in 1973. After grouting, many transverse joints opened again. Opened transverse joints and those without grouting accounted for 87% of the total area. Moreover, 70% of the major cracks, which were caused by the thermal stress from the hydration heat in the initial placed period, occurred after one to two years of placement. Approximately 30% of the cracks were produced by periodic temperature change and water pressure. Up until the end of 2000, cracks continued to develop in the dam.

During the operation period, the opening and closing of joints alternated with seasonal change. The surface joints downstream opened under low temperature and closed in high temperature, whereas the internal joints acted in an opposite manner. The horizontal joints downstream closed

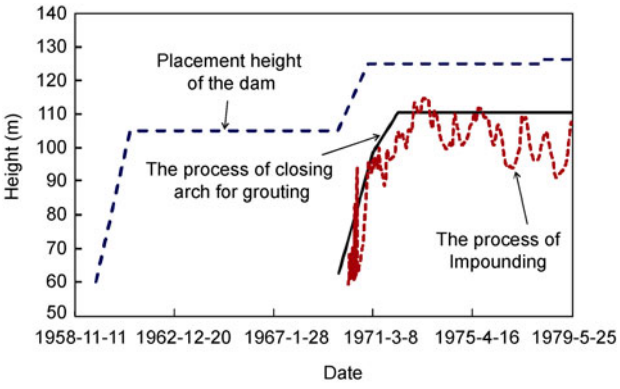

Figure 5 Process of placement, grouting, and impounding.

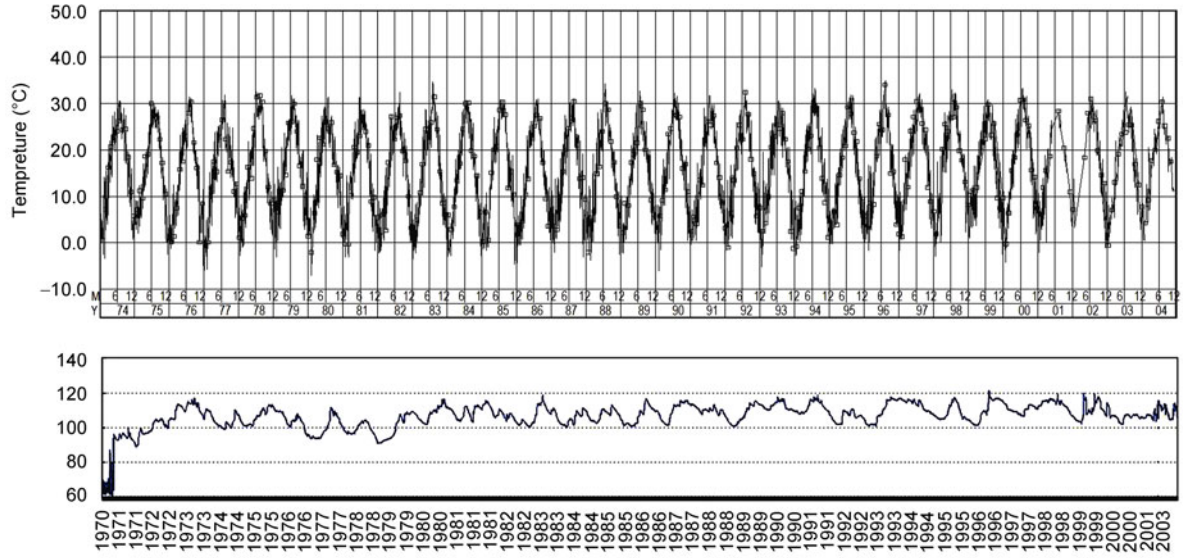

Figure 6 Observed temperature and water level for simulation.

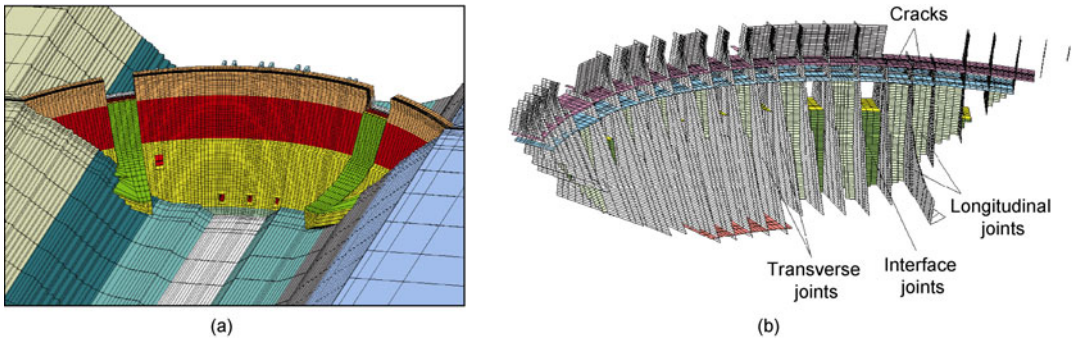

Figure 7 Diagram of the computation model. (a) Finite element mesh of the overall dam; (b) Transverse joints, longitudinal joints, and dam cracks.

Table 1 Thermodynamic parameters

Material	Elastic modulus (GPa)	Specific gravity (kg/m^3)	Poisson's ratio	Coefficient of temperature conductivity (m^2/h)	Specific heat (kJ/kg °C)	Coefficient of linear expansion
Rock	10	2450	0.2	0.00342	0.967	7
Concrete	16.5	2600	0.2	0.0050	0.978	10

Table 2 Strengths of joints set for simulation analysis

Types of joints	Tensile strength (MPa)	c (MPa)	ϕ (°)
Transverse joints before grouting	0	0	32
Transverse joints after grouting	0.8	1.0	36
Joint on interface of concrete in stage I & II	0.8	0.8	36
Assumed cracks (not cracked)	1.2	1.0	41

at high water level and opened at low level. Figure 9 shows the comparison between observed results and simulated results of the horizontal joints at EL105m of BL18, which are consistent with each other. These results show the tendency of the joints to open in winter and close in the summer, and increase in opening each year. This tendency is related to the fillers inside the joints.

5) Overall deformation of the dam

The distribution of temperature, stress, and displacement can be obtained through the simulation of the arch dam. Figure 10 shows the comparison between the observed and simulated results of radial displacement of the dam crest at BL18, which are consistent with each other. These results indicate that the analysis can reflect the real deformation of the dam. The deformation of the dam crest shows a tendency to increase upstream, which is related to the axial cracks on

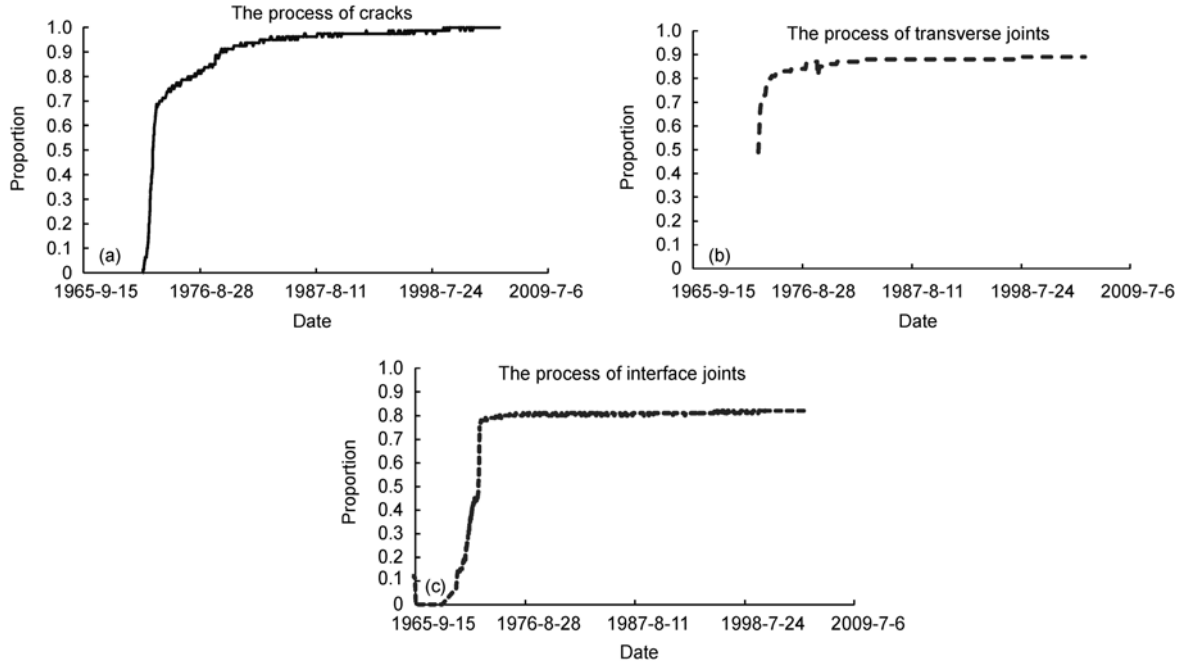

Figure 8 Area percentages of the formation of all cracks and joints with time. (a) Cracks; (b) transverse joints; (c) interface joints.

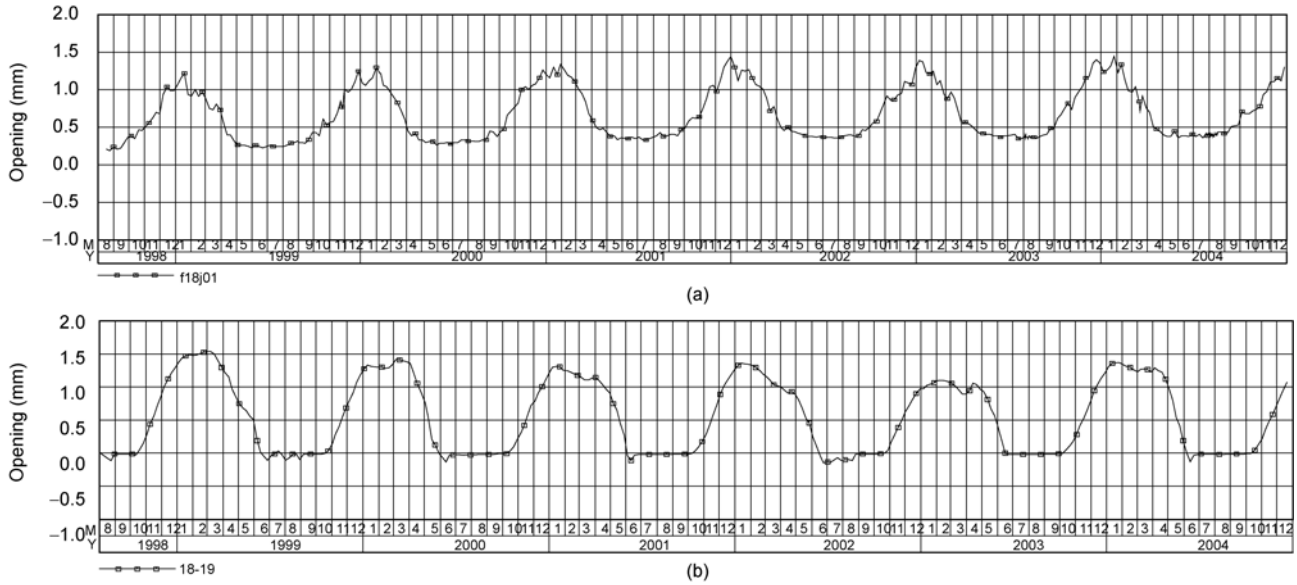

Figure 9 Comparison between observed results and simulated results of the opening-closing of one crack. (a) Observed process by joint meter; (b) simulation process.

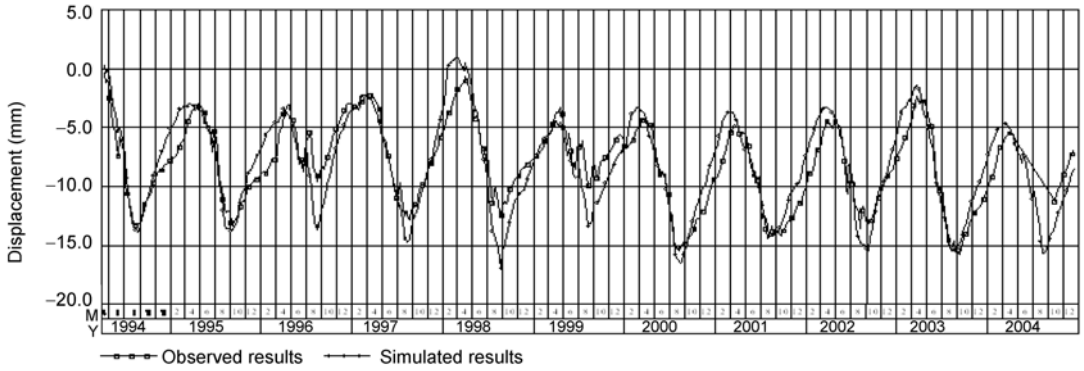

Figure 10 Comparison between the observed results and simulated results of displacement of the dam crest.

the dam crest.

The calculations for all cases were conducted, including the scenarios of no-opening of transverse joints after grouting and no interface joints. The results of the analysis show that the displacement toward the downstream of the overall dam increases at the downstream considering the joints. The reason for this is that the arch stiffness and overall stiffness are reduced by the joints, and the deformation toward the downstream increases at the downstream under water pressure.

4 Conclusions

Cracks and partial opening of transverse joints cannot be avoided in the construction and operation period of dams. Multi-defects can weaken the structural integrity and stiffness of the dam and have a strong effect on the working performance and safety degree of the dam. Simulation analysis considering all defects is an important method to study their long-term influence.

The numerical model of defects and the simulation method of high arch dam were discussed first in the current paper. A simulation analysis of the Chencun dam, from its placement in 1959–2004 through its 40-year operation, was then carried out. Finally, the process of transverse joints opening and crack formation, the opening of joint surface in stages I and II, and the influence of cracks on deformation and stress of the dam were studied. The results of the analysis show that the multi-defects caused larger deformation, periodic open-close caused cracks to develop inwards, and the increased loading on the beam caused higher tensile stress, increasing the risk of cracks at the dam heel. Therefore, the safety margin of the dam was reduced on the whole. Based on the simulation analysis, appropriate measures should be adopted to prevent the development of cracks, and observation and monitoring should be strengthened for the risks to be detected in a timely manner.

This work was supported by the National Key Technology R&D Program (Grant No. 2008BAB29B05), the National Natural Science Foundation of China (Grant No. 50909105), the Public Industry Research Special Funds of MWR (Grant No. 200801007) and the Research Special Funds of IWHR.

1 Li Z M. The pilot study of causes of cracks in puding RCC arch dam. J Hydroelectric Eng, 2001, 20(1): 96–102
2 Ru N H, Jiang Z S. Dam Failure and Safety Arch Dam. Beijing: China WaterPower Press, 1995
3 Zhu B F, Gao J Z, Chen Z Y, et al. Design and Research for Concrete Arch Dams. Beijing: China WaterPower Press, 2002
4 Li Z, Chen F, Zheng J B. Analysis and Study on Project and Major Technical Issues of Super-High Arch dam. Beijing: China Electric Power Publishing House, 2004
5 Ren Q W. Status quo and problems on safety analysis of high arch dam. J Hydraulic Eng, 2007, 37(Suppl.): 1023–1031
6 Ren Q W, Xu L Y, Wan Y H. Research advance in safety analysis methods for high concrete dam. Sci China Ser E-Tech Sci, 2007, 50(Suppl.): 62–78
7 Ngo D A. Network-Topological Approach to the Finite Element Analysis of Progressive Crack Growth in Concrete Members. Dissertation of Doctoral Degree. Berkeley: University of California, 1975. 845–862
8 Hillerborg A, Modeer M. Analysis of crack formation crack growth in concrete by means of fracture mechanics and finite elements. Cement Concrete Res, 1976, 6(6): 773–782
9 Bazant Z P, Cedolin L F. Fracture mechanics of reinforced concrete. J Eng Mesh Division, ASCE, 1980, 106(EM6): 1287–1306
10 Bao T F, Yu H. Detection of subcritical crack propagation for concrete dams. Sci China Ser E-Tech Sci, 2009, 52(12): 3654–3660
11 Goodman R E, Taylor R L. A Model for the Mechanics of Jointed Rock Proc ASCE, 1968, 94(3): 637–659
12 Yan S L, Wu D H, Huang Y Y. 3-D equivalent model of jointed rock masses considering the effects of joint face dilatancy. J Wuhan University Tech, 2000, 22(05): 100–103
13 Shi G H. Numerical Manifold Method and Discontinuous Deformation Analysis. Translated by Pei Juemin. Beijing: Tsinghua University Press, 1997
14 Zhu B F. Joint element with keys and the influence of joint on stresses in concrete dams. J Hydraulic Eng, 2001, 31(2): 1–7
15 Li X C, Cheng C H, Xu T. Study on non-integrity of arch dams. J Hydraulic Eng, 2002, 33(6): 47–52
16 Li J X, Wang G L, Jin F. Keys and the influence of joint on stresses in concrete dams. Water Power, 2001, 27(10): 45–48
17 Zhang G X, Liu Y, Zhou Q J. Study on real working performance and overload safety factor of high arch dam. Sci China Ser E-Tech Sci, 2008, 51(Suppl): 50–61
18 Long Y C, Zhou Y D, Zhang C H. A comparison study of nonlinear dynamic responses of arch dams based on two types of transverse joint models. J Hydraulic Eng, 2005, 36 (9): 80–85
19 Zhang B Y, Chen H Q, Tu J. Improved FEM based on dynamic contact force method for analyzing the stability of arch dam abutment. J Hydraulic Eng, 2004, 35(10): 9–14
20 Zhu B F. Theory and Application of Finite Element Method (the third version). Beijing: China WaterPower Press, 2009